

# Kinetics of the Thermal Degradation of Hyperbranched Poly(phenylene Sulfide)

Yan Bo, Chen Yanmo, You Hao, Sun Bin, Zhu Meifang

State Key Laboratory For Modification of Chemical Fibers and Polymer Materials, College of Material Science and Engineering, Donghua University, Shanghai 201620, People's Republic of China

Received 1 July 2007; accepted 30 March 2008

DOI 10.1002/app.28808

Published online in 6 November 2008 Wiley InterScience (www.interscience.wiley.com).

**ABSTRACT:** An advanced heat-resistant hyperbranched poly(phenylene sulfide) (HPPS) had been subjected to dynamic thermogravimetric analysis (TGA) in nitrogen. The presence of a single peak in the DTG curves suggested that weight loss occurs in a single stage. The thermal decomposition kinetics had been analyzed by applying the Kissinger, Friedman and Ozawa-Flynn methods. The  $E$  values determined for the hyperbranched PPS using these analyses were found to be 183.1, 189.2, 193.9 kJ mol<sup>-1</sup>,

respectively. Coats-Redfern method was used to discuss the probable degradation mechanisms. The solid-state decomposition mechanism followed by the degradation stage of HPPS was Phase boundary controlled mechanism ( $R_1$ ). © 2008 Wiley Periodicals, Inc. *J Appl Polym Sci* 111: 1900–1904, 2009

**Key words:** thermal degradation; hyperbranched poly(phenylene sulfide); kinetic

## INTRODUCTION

Dendritic polymer, including dendrimers and hyperbranched polymers, are a new class of 3D macromolecules, produced by multiplicative growth from small molecules that incorporate repetitive branching sequences but possess similar properties, such as high density of functional terminal groups and low-viscosity mainly due to a lack of restrictive inter-chain entanglements. Moreover, hyperbranched polymers are produced at a lower cost and are much easier to process than dendrimers. Properties of dendritic polymers in solution, molten and in solid-state are considerably different from those of linear polymers, because of their specific molecular structure and their large number of end groups.<sup>1</sup>

In recent years, considerable attention was devoted to the synthesis of branched polymers and setting up a relationship between their structure and properties.<sup>2–7</sup> There have been a few studies examining the degradation of hyperbranched polymers.<sup>8–10</sup> Thermal degradation of linear poly(phenylene sulfide) was frequently investigated.<sup>11–17</sup> However, one cannot find articles in the literature that discuss ther-

mal degradation of hyperbranched poly(phenylene sulfide).

In this article, the thermal degradation of hyperbranched poly(phenylene sulfide) (HPPS) was investigated with dynamic thermogravimetric analysis (TGA). One objective was to investigate the kinetics of the thermal degradation of HPPS using different kinetic methods. The other objective was to investigate the thermal degradation mechanism as a solid-state process. The kinetic parameters, obtained from different kinetic methods were compared and discussed.

## EXPERIMENTAL

### Materials

All reagents used are of analytical grade. The following products are used as received: 2,4-dichlorobenzothiol (Shou and Fu Chemical Company, Zhejiang, China) and *N*-methyl-2-pyrrolidinone (NMP) (China National Group Corp. of Medicine, Shanghai, China).

### Synthesis of HPPS

The synthesis procedure of HPPS in this work was similar to that in Hanson's work<sup>5</sup> and Hewen Liu's work.<sup>18</sup> To improve monomer conversion, we decreased reaction temperature and NMP was used as the reaction medium. A 250-mL three-neck flask was charged with NMP 80 mL, 2,4-dichlorobenzothiol 10 g and KOH 5.6 g. The mixture was stirred

Correspondence to: C. Yanmo (ymc@dhu.edu.cn) or Z. Meifang (zhumf@dhu.edu.cn).

Contract grant sponsor: National High Tech 863 project; contract grant number: 2006AA03Z550.

Contract grant sponsor: Enterprise Funding; contract grant number: 2005042.

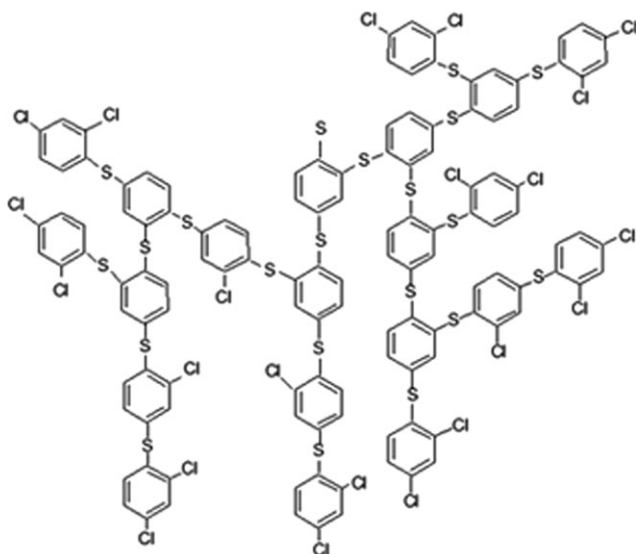


**Figure 1** The structure of HPPS.

under pure  $N_2$  and was heated and maintained 10 h. The reactions were then cooled and diluted with an equal volume of water and poured into 300 mL 10% HCl solution. The resulting precipitate was vacuum-dried at  $160^\circ\text{C}$  and then dissolved with vigorous stirring in a minimal amount of THF. The THF solution was added drop wise to hexanes with vigorous stirring over a period of 2 h. This precipitate was then filtered, washed with hexanes, and dried thoroughly under vacuum. The product obtained as yellow powder. The structure of HPPS was illustrated in Figure 1. FTIR (KBr): 3051, 1565, 1449, 1365, 1095, 1029, 868, 810  $\text{cm}^{-1}$  and  $^1\text{H NMR}$  ( $\text{CD}_3\text{Cl}$ ) 7.47, 7.43, 7.39, 7.37, 7.26, 7.22 ppm. In the  $\text{AB}_2$  systems, the degree of branching determined by NMR was usually about 50–60%.<sup>2–4</sup> However, for the hyperbranched PPS, the degree of branching could not be determined from its  $^1\text{H NMR}$  spectrum because the chemical shifts of the aromatic protons were not well resolved for this determination.<sup>5,6</sup>

### Thermogravimetric analysis

TGA was done with a NETZSCH TG-209-F1 thermogravimetric analyzer. Conventional constant heating rate TGA measurements were run at 5, 10, 20, and  $40^\circ\text{C}/\text{min}$  in nitrogen with the sample size about 8–10 mg to provide a control set of values for thermal decomposition parameters. The nitrogen flow was 30 mL/min.

### Kissinger method<sup>16</sup>

The Kissinger method is based on the calculation of the apparent activation energy  $E$  on the temperature at which the maximum rate of weight loss,  $T_m$  occurs in the DTG curve at several rates. The Kissinger equation is

$$\ln\left(\frac{\beta}{T_m^2}\right) = \ln\left[A n(1-X)_m^{-1}\right] - \left(\frac{E}{RT_m}\right) \quad (1)$$

Where  $\beta$  is the heating rate,  $A$  is the pre-exponential factor,  $n$  is the order of the reaction and  $R$  is the universal gas constant. A plot of  $\ln(\beta/T_m^2)$  versus  $(1/T_m)$  then gives  $E/R$  from the slope of the line.

### Friedman method<sup>19,20</sup>

Friedman method is a differential method. It is independent of thermal degradation mechanism and is used most widely. Friedman method is

$$\ln\frac{dX}{dt} = \ln\left(\beta\frac{dX}{dT}\right) = \ln[Af(X)] - \frac{E}{RT} \quad (2)$$

This method requires several thermograms to obtain heating rate. By plotting  $\ln(dX/dt)$  against  $1/T$  at constant values of  $X$  obtain from each thermogram, a set of straight line can be obtained. The slope of each line is  $-E/R$ , and the intercept is  $\ln[Af(X)]$ .

**TABLE I**  
Algebraic Expressions for  $g(X)$  for the Most Frequently Used Mechanisms of Solid-State Processes<sup>24</sup>

Symbol	$g(X)$	Solid-state processes
$A_2$	$[-\ln(1-X)]^2$	Nucleation and growth (Avrami equation 1)
$A_3$	$[-\ln(1-X)]^3$	Nucleation and growth (Avrami equation 2)
$A_4$	$[-\ln(1-X)]^4$	Nucleation and growth (Avrami equation 3)
$R_1$	$X$	Phase boundary controlled (one-dimensional movement)
$R_2$	$2[1 - \ln(1-X)]^{1/2}$	Phase boundary controlled (contracting area)
$R_3$	$3[1 - \ln(1-X)]^{1/3}$	Phase boundary controlled (contracting volume)
$D_1$	$X^2$	One-dimensional diffusion
$D_2$	$(1-X)\ln(1-X) + X$	Two-dimensional diffusion (Valensi equation)
$D_3$	$[1 - (1-X)^{1/3}]^2$	Two-dimensional diffusion (Jander equation)
$D_4$	$[1 - (2/3)X] - (1-X)^{2/3}$	Three-dimensional diffusion (Ginstling-Brounshtein equation)
$F_1$	$-\ln(1-X)$	Random nucleation with one nucleus on the individual particle
$F_2$	$(1-X)^{-1}$	Random nucleation with two nuclei on the individual particle
$F_3$	$(1-X)^{-2}$	Random nucleation with three nuclei on the individual particle

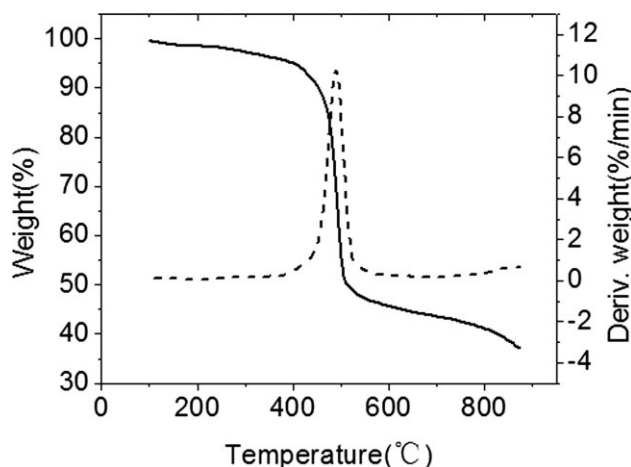


**Figure 2** The TGA and DTG curves of HPPS heated at rate 10°C/min.

### Flynn -Wall-Ozawa method<sup>21</sup>

This method is based on the representation of the degradation reaction by power law kinetics. This method used the approximation of Doyle to evaluate the integrated form of the rate equation and yields eq. (3) as an approximate solution. Assuming  $E/RT > 20$ , it can be obtained:

$$\log(\beta) = \log \frac{AE}{g(X)R} - 2.315 - \frac{0.4567 E}{RT} \quad (3)$$

where  $g(X)$  represents the weight loss function.  $E$  is obtain from a plot of  $\log(\beta)$  versus  $1/T$  for fixed degrees of conversion and the slope of the line is given by  $-0.4567E/R$ .

### Coats-Redfern method<sup>22,23</sup>

The Coats-Redfern method uses an asymptotic approximation for the resolution as follow at different conversion values. If  $(2RT)/T \rightarrow 0$  is true for the Doyle approximation, a natural logarithmic form can be obtained:

$$\log \frac{g(X)}{T^2} = \ln \frac{AR}{\beta E} - \frac{E}{RT} \quad (4)$$

According to the different degradation processes, with the theoretical function  $g(X)$  being listed in Table I,  $E$  and  $A$  can be obtained from the plot of  $\ln[g(X)/T^2]$  versus  $1/T$ , as well as the valid reaction mechanism.

## RESULTS AND DISCUSSION

### Thermal stability

Typical curves for TGA and derivative thermogravimetry (DTG) of the HPPS in nitrogen at heating

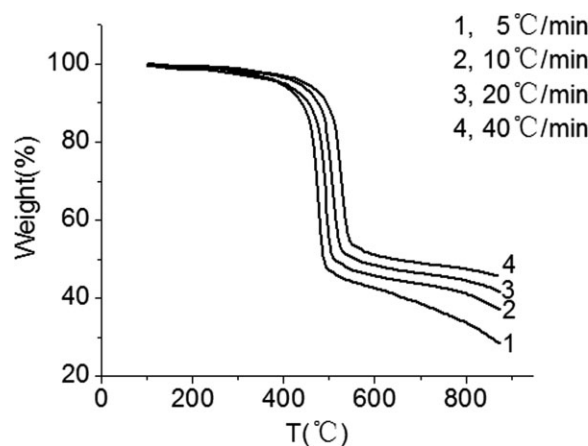


**Figure 3** The TGA curves of HPPS heated at rate from 5°C/min to 40°C/min.

rates of 10°C/min are shown in Figure 2. The presence of a single peak in the DTG cures suggest that weight loss occurs in a single stage. The TGA cures of the HPPS at heating rates of 5, 10, 20, and 40°C/min are shown in Figure 3. As the heating rate is increased, the degradation temperature ( $T_d$ ) moves to higher temperature. The change from 476°C for 5°C/min to 529°C for 40°C/min. The char yield at 1123 K increases significantly with increasing heating rate. The change from 28.2% for 5°C/min to 45.4% for 40°C/min. The results are summarized in Table II.

### Kinetics of thermal decomposition

The Kissinger method bases the calculation of the apparent activation energy  $E$  on the temperature at which the maximum rate of weight loss. Figure 4 shows the relationship given by eq.(1) of Kissinger method. A good linear relationship for each heating rate is obtained. A plot of  $\ln(\beta/T_m^2)$  versus  $(1/T_m)$  then gives  $E$  from the slope of the line. The activation energies calculated from the slopes are shown in Table III. The calculated  $E$  value of HPPS is 183.1 k Jmol<sup>-1</sup>.

The Friedman method is a differential method. It is independent of thermal degradation mechanism and is used most widely. The Friedman method is based on eq.(2) and requires several thermograms at different heating rate. Figure 5 illustrate the plots of  $\ln(\beta dX/dT)$  against  $1000/T$  at varying conversion. A set of straight lines is obtained at different

**TABLE II**  
Thermal Decomposition Dates of HPPS

Heating rate (°C/min)	5	10	20	40
$T_d$ (°C)	476	491	510	529
Char yield (%)	28.2	36.8	41.6	45.4

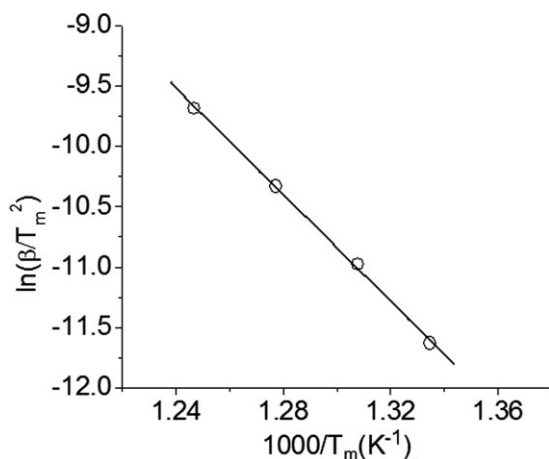


Figure 4 Kissinger plots of HPPS.

conversion, with the slope of each line being  $-E/R$ . The values of activation energies are determined from the slopes of the plots are shown in Table III. The mean values of  $E$  of HPPS is  $189.2 \text{ kJ mol}^{-1}$ .

Flynn–Wall–Ozawa method is an integral method, which is also independent of the degradation mechanism. Equation (3) is used, and the activation energy of HPPS is obtained from plot of  $\log(\beta)$  against  $1000/T$  at a fix conversion with the slope of such a line being  $-0.4567E/RT$ . Figure 6 illustrate the plots of  $\log(\beta)$  versus  $1000/T$  at varying conversion ( $X$ ). The activation energies calculated from the slopes are shown in Table III. The mean value of  $E$  is  $193.9 \text{ kJ mol}^{-1}$ .

Table III shows that the values of  $E$  are constant with increasing degree of conversion. Through analyzing the activation energies obtained by the three methods, it is found that the values are close to each other for Kissinger method, Friedman method and Flynn–Wall–Ozawa method.

#### Determination of kinetic mechanism of HPPS

To investigate the solid-state processes for the thermal degradation of HPPS, Coats–Redern method is chosen, as it does not require previous knowledge of

TABLE III  
Kinetic Parameters for Hyperbranched PPS Degradation by Different Methods

Method	Friedman	Flynn–Wall–Ozawa	Kissinger
Degree of conversion	$E \text{ (kJ mol}^{-1}\text{)}$	$E \text{ (kJ mol}^{-1}\text{)}$	$E \text{ (kJ mol}^{-1}\text{)}$
0.2	$176.4 \pm 9.0$	$193.1 \pm 11.2$	$183.1 \pm 4.4$
0.3	$178.4 \pm 7.6$	$192.6 \pm 9.7$	
0.4	$173.8 \pm 4.4$	$198.3 \pm 9.8$	
0.5	$175.1 \pm 6.2$	$193.9 \pm 2.6$	
0.6	$193.5 \pm 14.9$	$192.6 \pm 5.2$	
0.7	$237.7 \pm 29.7$	$193.1 \pm 12.1$	

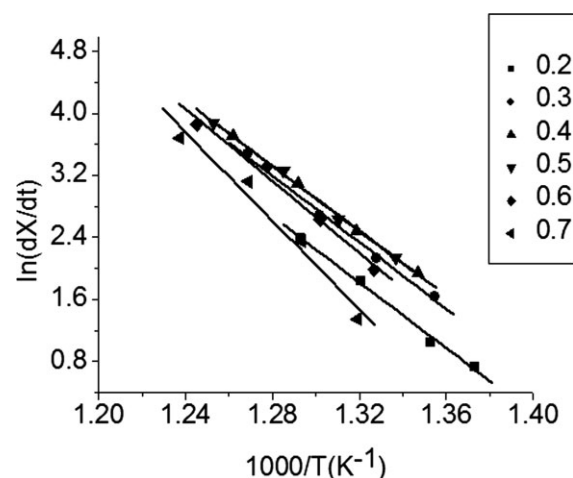


Figure 5 Friedman plots of HPPS at varying conversion.

the reaction mechanism for determining the activation energy. Some authors have used the activation energies obtained by this method to check their thermal degradation mechanism models.<sup>23,25,26</sup>

According to eq.(4), activation energy for every  $g(X)$  function listed in Table I can be calculated at constant heating rates from fitting of  $\ln[g(X)/T^2]$  versus  $1/T$ . The same conversion values are used in this case just as in Flynn–Wall–Ozawa method. The activation energies and the correlations at a constant heating rate ( $10 \text{ K/min}$ ), for the degradation processes, are tabulated in Table IV. Comparing the values of activation energies in Table IV, it is found that the activation energy corresponding to a mechanism  $R_1$  is  $183.7 \text{ kJ mol}^{-1}$ , is in better agreement with that obtained using Kissinger method ( $183.1 \text{ kJ mol}^{-1}$ ), Friedman method ( $189.2 \text{ kJ mol}^{-1}$ ) and Flynn–Wall–Ozawa method ( $193.9 \text{ kJ mol}^{-1}$ ). These faces strongly suggest that the solid-state thermal degradation mechanism followed by HPPS is a phase boundary controlled reaction mechanism ( $R_1$ ).

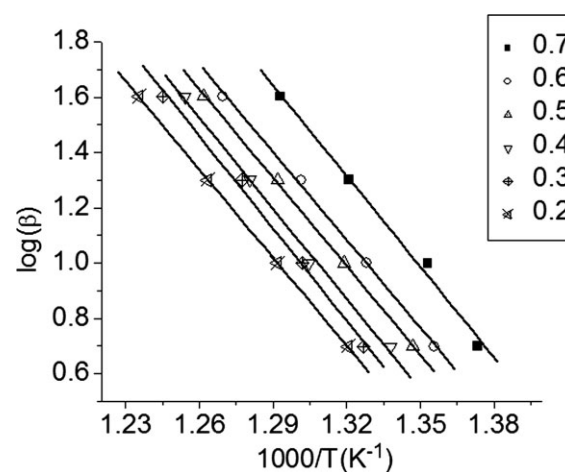


Figure 6 Flynn–Wall–Ozawa plots of HPPS at varying conversion.



TABLE IV  
Activation Energies of HPPS Obtained from the  
Coats-Redfern Method for Several Solid-State  
Process at 10 K/min

Mechanism	$g(X)$	$E$ (kJ mol <sup>-1</sup> )	R
A <sub>2</sub>	$[-\ln(1 - X)]^2$	493.5 ± 31.3	0.9920
A <sub>3</sub>	$[-\ln(1 - X)]^3$	288.1 ± 69.1	0.9016
A <sub>4</sub>	$[-\ln(1 - X)]^4$	999.6 ± 62.7	0.9922
R <sub>1</sub>	$X$	183.7 ± 8.03	0.9962
R <sub>2</sub>	$2[1 - \ln(1 - X)]^{1/2}$	271.9 ± 47.4	0.9252
R <sub>3</sub>	$3[1 - \ln(1 - X)]^{1/3}$	480.1 ± 65.1	0.9286
D <sub>1</sub>	$X^2$	378.6 ± 16.1	0.9964
D <sub>2</sub>	$(1 - X) \ln(1 - X) + X$	413.2 ± 20.2	0.9952
D <sub>3</sub>	$[1 - (1 - X)^{1/3}]^2$	452.6 ± 25.5	0.9937
D <sub>4</sub>	$[1 - 2X/3] - (1 - X)^{2/3}$	426.3 ± 21.9	0.9947

The thermal degradation mechanism of the Fortron 205 PPS sample is R<sub>3</sub> and the Ryton P-4 PPS sample is R<sub>2</sub><sup>16</sup>. The Fortron PPS sample is believed to possess less chain-branching than the Ryton PPS sample.<sup>27</sup> It seems that because of the branch chain, the thermal degradation mechanism of PPS changed from R<sub>3</sub> to R<sub>2</sub>. Because the hyperbranched polymers have much more branch chains, that the thermal degradation mechanism of HPPS is R<sub>1</sub> is reasonable.

### CONCLUSIONS

The thermal degradation parameters of hyperbranched poly(phenylene sulfide) samples have been measured by TGA. The presence of a single peak in the DTG curves suggest that weight loss occurs in a single stage. The results show that the activation energies by Kissinger, Friedman, Flynn-Wall-Ozawa methods are 183.1, 189.2, 193.9 kJ mol<sup>-1</sup>, respectively. The analyses of the results obtained by Coat-Redfern methods shows that the solid-state process for the degradation stage of HPPS follow a Phase

boundary control mechanism (R<sub>1</sub>), with integral form  $g(X) = X$ .

### References

1. Voit, B. *J Polym Sci Part A Polym Chem* 2000, 38, 2505.
2. Kim, Y. H.; Webster, O. W. *Macromolecules* 1992, 25, 5561.
3. Turner, S. R.; Walter, F.; Voit, B. I.; Mourey, T. H. *Macromolecules* 1994, 27, 1611.
4. Feast, W. J.; Stainton, N. M. J. *Mater Chem* 1995, 5, 405.
5. Mellace, A.; Hanson, J. E.; Griepenburg, J. *Chem Mater* 2005, 17, 1812.
6. Uhrich, K. E.; Hawker, C. J.; Fréchet, J. M. *Macromolecules* 1992, 25, 4583.
7. Mezei, A.; Meszaros, R.; Varga, I.; Gilanyi, T.; *Langmuir* 2007, 23, 4237.
8. Vukovic, J.; Steinmeier, D.; Lechner, M. D.; Jovanovic, S.; Bozic, B. *Polym Degrad Stab* 2006, 91, 1903.
9. Hanssani, M. L. *J Appl Polym Sci* 2006, 101, 2079.
10. Wang, Q. F.; Shi, W. F. *Polym Degrad Stab* 2006, 91, 1289.
11. Christopher, N. S. J.; Cotter, J. L.; Knight, G. J.; Wright, W. W. *J Appl Polym Sci* 1968, 12, 863.
12. Peters, O. A.; Still, R. H. *Polym Degrad Stab* 1993, 42, 41.
13. Zebger, I.; Elorza, A. L.; Salado, J.; Alcala, A. G.; Goncalves, E. S.; Ogilby, P. R. *Polym Degrad Stab* 2005, 90, 67.
14. Li, X. G.; Huang, M. R.; Bai, H.; Yang, Y. L. *J Appl Polym Sci* 2002, 83, 2053.
15. Perng, L. H. *Polym Degrad Stab* 2000, 69, 323.
16. Day, M.; Budgell, D. R. *Thermochim Acta* 1992, 203, 465.
17. Budgell, D. R.; Day, M.; Cooney, J. D. *Polym Degrad Stab* 1994, 43, 109.
18. Xu, R. L.; Liu, H. W.; Shi, W. F. *J Polym Sci Part B: Polymer Phys* 2006, 44, 826.
19. Yang, M. H. *J Appl Polym Sci* 2002, 86, 1540.
20. Li, X. G.; Huang, M. R. *Polym Degrad Stab* 1999, 64, 81.
21. Popescu, C. *Thermochim Acta* 1996, 285, 309.
22. Coats, A. W.; Redfern, J. P. *Nature* 1964, 201, 68.
23. Sun, J. T.; Huang, Y. D.; Gong, G. F.; Cao, H. L. *Polym Degrad Stab* 2006, 91, 339.
24. Phadnis, A. B.; Deshpande, V. V. *Thermochim Acta* 1983, 62, 361.
25. Nùñez, L.; Fraga, M. R. *Polymer* 2000, 41, 4635.
26. Monterrat, S.; Mälek, J. *Thermochim Acta* 1998, 313, 83.
27. Hou, C. S. H.; Zhao, B. C. H.; Yang, J.; Yu, Z. L.; Wu, Q. X. *J Appl Polym Sci* 1995, 56, 581.